

DEVELOPING MULTIPLE-FREQUENCY DISCRIMINANTS FOR USE WITH REGIONAL CODA-AMPLITUDE MEASUREMENTS

C. K. Saikia<sup>1</sup>, K. Mayeda<sup>2</sup>, L. Zhu<sup>3</sup>, and R. B. Herrmann<sup>3</sup>

URS Group, Inc.<sup>1</sup>, Lawrence Livermore National Laboratory<sup>2</sup>, and Saint Louis University<sup>3</sup>

Contract Nos. DE-AC52-04NA225545<sup>1</sup>, DE-FC52-04NA25546<sup>3</sup>, and W-7405-ENG-48<sup>2</sup>

**ABSTRACT**

This is a collaborative study involving three institutions to investigate the feasibility of employing regional coda-wave amplitude measurements in multiple narrow pass bands for the purpose of discriminating small, regionally recorded seismic events. The motivation comes from previous studies that have shown that regional, single-station coda-magnitude estimates are more stable and accurate than any direct phase measure to date (e.g., Mayeda et al., 2003a,b). Typically, the source amplitude estimates derived from the coda have inter-station variances on the order of 0.07 log amplitude units; hence the method is excellent for regions with sparse station coverage. The method has been tested over large geographic regions spanning both local and regional distances for the purpose of magnitude estimation (e.g., Phillips et al., 2003; Mayeda et al., 2003; Eken et al., 2003; Morasca et al., 2003). In terms of the discrimination, only a preliminary study using coda waves was performed on Nevada Test Site (NTS) explosions and earthquakes in the study by Walter et al. (2003). Due to the nature of the coda, path and azimuthal source-radiation effects are averaged over, making coda amplitudes insensitive to local structure, in sharp contrast to direct regional phases such as Pn, Pg, and Lg. Calibrated to seismic moment ( $M_0$ ), or moment magnitude ( $M_w$ ), coda-derived source spectra provide a means to obtain moment estimates from smaller or more distant events, which cannot be analyzed with conventional waveform or spectral source-inversion techniques because of signal-to-noise limitations.

So far, we made progress in obtaining  $M_0$  and  $M_w$  of small magnitude earthquakes that have occurred in Korea and China using regional seismograms recorded by the in-country stations. Tying  $M_w$  (coda magnitude) to  $M_w$  (moment magnitude) also provides a physical measure of event size, which is unbiased, i.e., transportable. However, shallow events ( $h < 3$  km) of all source types have pronounced peaks in their spectra in the 0.2–1.0 Hz range, relative to normal-depth earthquakes due to the Rg-to-S conversion. These source-spectra differences need to be accounted for to make direct coda-amplitude comparisons with normal-depth earthquakes, particularly for discrimination purposes. Without doing so, shallow events will tend to have their long-period source spectrum overestimated. To facilitate  $M_w$  (coda magnitude) vs.  $M_w$  (moment magnitude) comparison, we established focal mechanisms, depths and seismic moments for a small subset of earthquakes occurring in the Korean Peninsula and in its adjoining eastern and western seas. Similar studies have also been undertaken for estimating  $M_0$  (seismic moment) and  $M_w$  (moment magnitude) for Chinese earthquakes by modeling regional seismograms. We have also completed a study related to earthquakes in southwestern United States (US). Thus, we have established accurate source depth and seismic moments needed for the calibration of the regional coda amplitude in our study region. To add to our dataset, we have also collected regional waveforms recorded by stations of three temporary PASSCAL networks operated in Nepal, Bhutan, and Nanga Parbat so that decay of the coda amplitudes can be calibrated to many regions of the world.

### OBJECTIVE

The objective of this study is to investigate how to best employ multiple-frequency coda-amplitude measurements to identify source type, i.e., discriminate seismic events. To do so, we take advantage of the known differences in coda source-spectra characteristics between normal depth earthquakes and shallow events, particularly explosions. To this end, our objective is to apply the analysis to events occurring in the southwest US and then calibrate the Korean Peninsula, China, Nepal, and Nanga Parbat by analyzing regional seismograms. That work requires estimating seismic moment ( $M_o$ ) and moment-magnitude ( $M_w$ ) from small magnitude earthquakes.

We make coda-amplitude measurements and compare them with those measured from the Lg waves (Figure 1) (Mayeda et al., 2003a,b). This illustrates that coda methodology works well, including across the tectonic regions. Data plotted in this example were obtained by applying the method to broadband data from 50 earthquakes ( $4.0 < M_w < 7.6$ ) distributed over the entire region of Turkey. The upper left panel shows distance corrected-coda amplitude measurements from the stations ISP and ISKB using signals in the frequency band 0.1–0.2 Hz. The direct Lg waves amplitude measurements in the same frequency band between these two stations are shown in the right. Clearly, the direct Lg wave amplitude measurements have larger scatter in the range of 0.27 to 0.45. This indicates that the inter-station scatter in the distance-corrected coda-amplitude measurements is remarkably 3-to-4 times lower than those obtained from the distance-corrected direct Lg waves. Once we complete the entire data collection, the objective is to undertake a similar study to establish how well inter-station coda amplitude behaves relative to Lg waves in our study region.

### RESEARCH ACCOMPLISHED

Figure 2 shows the distribution of stations of the KMA and KIGAM seismic networks in the Korean Peninsula, including the locations of 171 earthquakes that occurred in and around the Korean Peninsula. We have collected regional seismograms from these events and organized and binned them according to magnitude. Although the seismic networks have many stations, we have waveforms from only a limited number of stations for each event. Using these regional data, our team member Prof. R. B. Herrmann has determined focal mechanisms, depths, and seismic moments of nine earthquakes ( $3.4 < M_w < 3.8$ ). The modeling study is still on-going, and we are selecting events that have suitable seismograms for the purpose.

We also collected regional seismograms recorded by the stations of the Chinese National Digital Seismic Network (CNDSN, Figure 3). This network had started several years ago by the Chinese Seismological Bureau and covers the entire mainland China. Seismograms from some events are available to our team member who is modeling regional seismograms to develop crustal models for different parts of China. The top panel in Figure 4 shows the epicenter of a  $M_w$  5 aftershock of the 2001 Kunlun earthquake. Triangles represent the locations of the nearby stations of the CNDSN. The bottom panel in the figure shows an example of the on-going modeling study where the solid dark traces correspond to the recorded seismograms, and thin red traces on top of the dark traces correspond to the synthetic seismograms predicted using the best fitting focal mechanism. Here we show the  $P_{nl}$  seismograms in the first two columns and the long-period surface waves of the vertical, radial, and tangential components in the next three columns, respectively. The velocity model used in the inversion was taken from the Tibet region. The top number beneath each waveform pair (data and synthetic) for each segment represents the time shift that is allowed in fitting the data. The bottom number corresponds to the estimate of the cross-correlation coefficient between the two data traces times 100. So far, regional seismograms from 15 events have been successfully modeled and their seismic moment ( $M_o$ ) and moment-magnitude ( $M_w$ ) have been tabulated.

Because of the restrictive nature of the Chinese data set Dr. Zhu himself visited URS Group, Inc., to measure the coda and Lg amplitudes at multiple frequency bands as previously selected by Dr. Kevin Mayeda of Lawrence Livermore National Laboratory. To this end, we have completed an analysis of events recorded at stations HTA, HTG, KSH, and WUS. Figure 5 shows examples of the envelopes processed at different frequency bands that have been used in the measurement of the coda amplitude.

In addition to these data, we have collected regional waveforms from the Nanga Parbat PASSCAL experiment in northern Himalaya. Researchers at Lamont Doherty Observatory have already determined the locations of many of the events recorded by this network and we used their catalog to download seismograms from the IRIS database.

## 27th Seismic Research Review: Ground-Based Nuclear Explosion Monitoring Technologies

The events have occurred in the Himalayan mountain region and are recorded between 250 and 500 km by multiple stations. Because of the complex geology of the region, we expect these data to provide a good test bed for testing the robust behavior of the coda-wave measurements vs the Lg wave amplitude measurements.

We have also employed a modified version of Mayeda et al. (2003a,b) coda-magnitude method in which an additional distance term is incorporated into the empirical magnitude relationship. This was applied to a dataset compiled for events occurring in the southwestern United States. Figure 6 is a map showing the stations and events used. Unlike the multiple bands, we used only one passband that of a worldwide station network short-period instrument, and measured the coda magnitude instead of the coda amplitude. The upper-left panel in Figure 7 compares single-station (PAS)  $M_w$  (coda) values to those determined from the waveform and spectral inversion source studies; a fairly small standard error of 0.09 is achieved. The upper-right and lower-left panels provide inter-station  $M_w$  comparisons. The lower-right panel shows network averaged  $M_w$  (coda) vs. the best estimate of  $M_w$  from source inversion studies. There is a slight depression in  $M_w$ (coda) values for the larger ( $M_w > 6.5$ ) events, which is believed to be due to post-corer-frequency spectral fall-off in the coda measurements.

### CONCLUSIONS

The on-going study investigates the feasibility of employing regional coda-wave amplitude measurements in multiple narrow pass bands for the purpose of discriminating small, regionally recorded seismic events. Collection of data for this purpose is a continued effort and we have collected a major amount of data from different tectonic areas, including the main focus regions in Korea and parts of China. So far, we have completed waveform modeling to establish seismic moment and moment-magnitude ( $M_w$ ) for several earthquakes from Korea and China.

### REFERENCES

- Eken, T, K. Mayeda, A. Hofstetter, R. Gok, N. Turkelli, and G. Orgulu (2003), An Application of the Coda Methodology for Moment-Rate Spectra Using Broadband Stations in Turkey, submitted to *Geophys. Res. Lett.*
- Hartse, H. W., W. S. Phillips, M. C. Fehler, and L. S. House (1995), Single-Station Spectral Discrimination Using Coda Waves, *Bull. Seism. Soc. Am.* 85: 1464–1474.
- Mayeda, K., A. Hofstetter, J. O’Boyle, and W. R. Walter (2003a), Stable and Transportable Regional Magnitudes Based on Coda-Derived Moment-Rate Spectra, *Bull. Seism. Soc. Am.* 93: 224–239.
- Mayeda, K., T. Eken, A. Hofstetter, N. Turkelli, J. O’Boyle, G. Orgulu, and R. Gok (2003b), Moment Magnitude Calibration for the Eastern Mediterranean Region from Broadband Regional Coda Envelopes, in *Proceedings of the 25th Seismic Research Symposium—Nuclear Explosion Monitoring: Building the Knowledge Base*, LA-UR-03-6029, Vol. 1, pp. 420–427.
- Morasca, P., K. Mayeda, L. Malagnini, and W. R. Walter (2003), Coda-Derived Source Spectra, Moment Magnitudes, and Energy-Moment Scaling in the Western Alps, submitted to *Geophys. J. Int.*
- Phillips, W. S., H. J., Patton, C. M. Aprea, H. E. Hartse, G. E. Randall, and S. R. Taylor (2003), Automated Broad Area Calibration for Coda Based Magnitude and Yield, in *Proceedings of the 25th Seismic Research Review—Nuclear Explosion Monitoring: Building the Knowledge Base*, LA-UR-03-6029, Vol. 1, pp. 437–444.
- Walter, W. R., M. E. Pasyanos, A. J. Rodgers, K. M. Mayeda, and A. Sicherman (2003), Regional Body-Wave and Surface-Wave Tomography Models to Improve Discrimination, in *Proceedings of the 25th Seismic Research Review—Nuclear Explosion Monitoring: Building the Knowledge Base*, LA-UR-03-6029, Vol. 1, pp. 495–503.

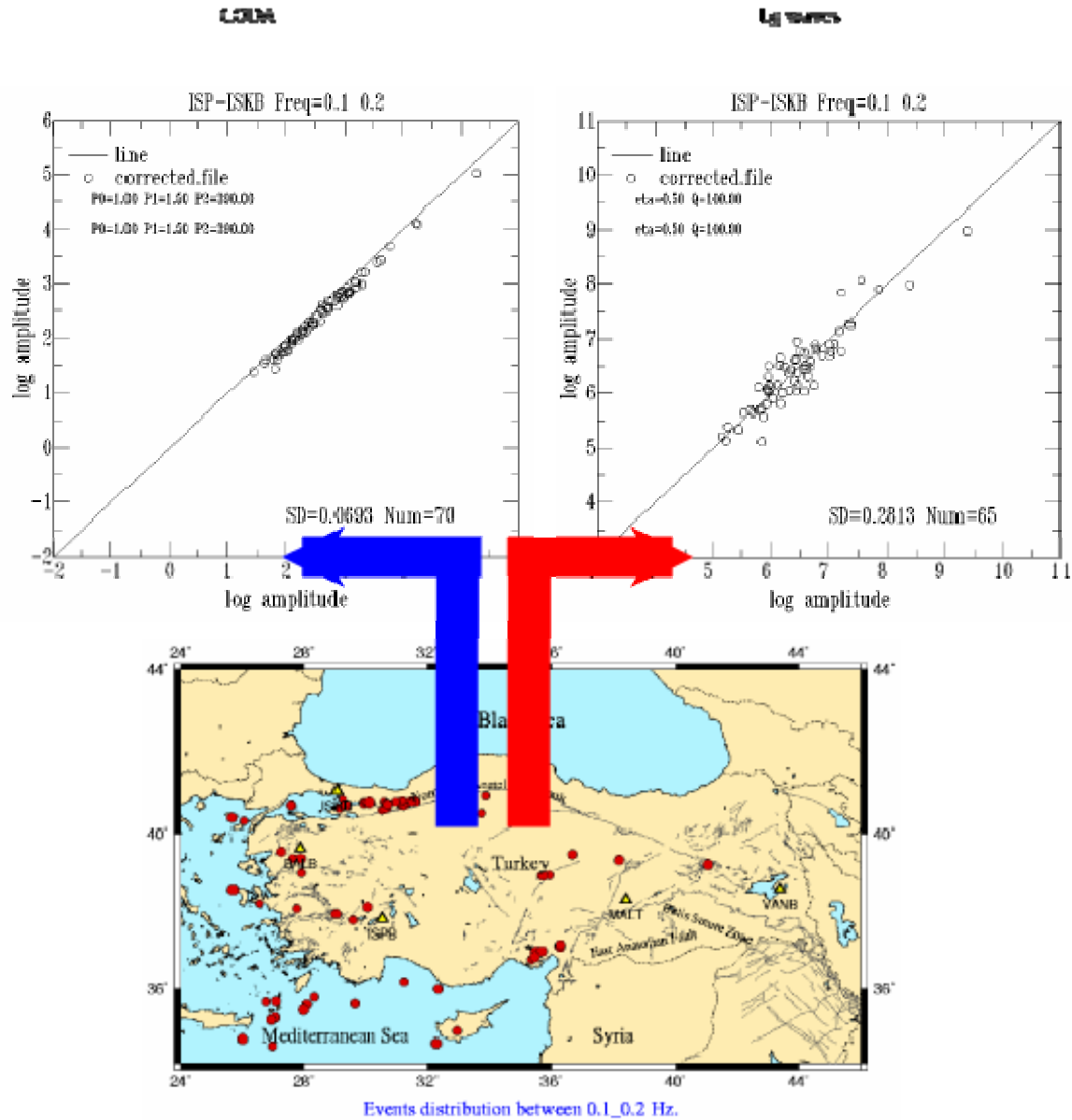


Figure 1. Illustration of transportability of the coda method. Plotted are the measurements of the distance-corrected coda amplitude (upper left panel) and direct Lg wave amplitudes (right panel) at stations ISP and ISKB in the frequency band 0.1–0.2 Hz. The inter-station standard deviation results show that coda amplitudes at this frequency band are four times more stable than distance corrected direct Lg waves using common events in the map shown at the bottom (taken from Mayeda et al., 2003).

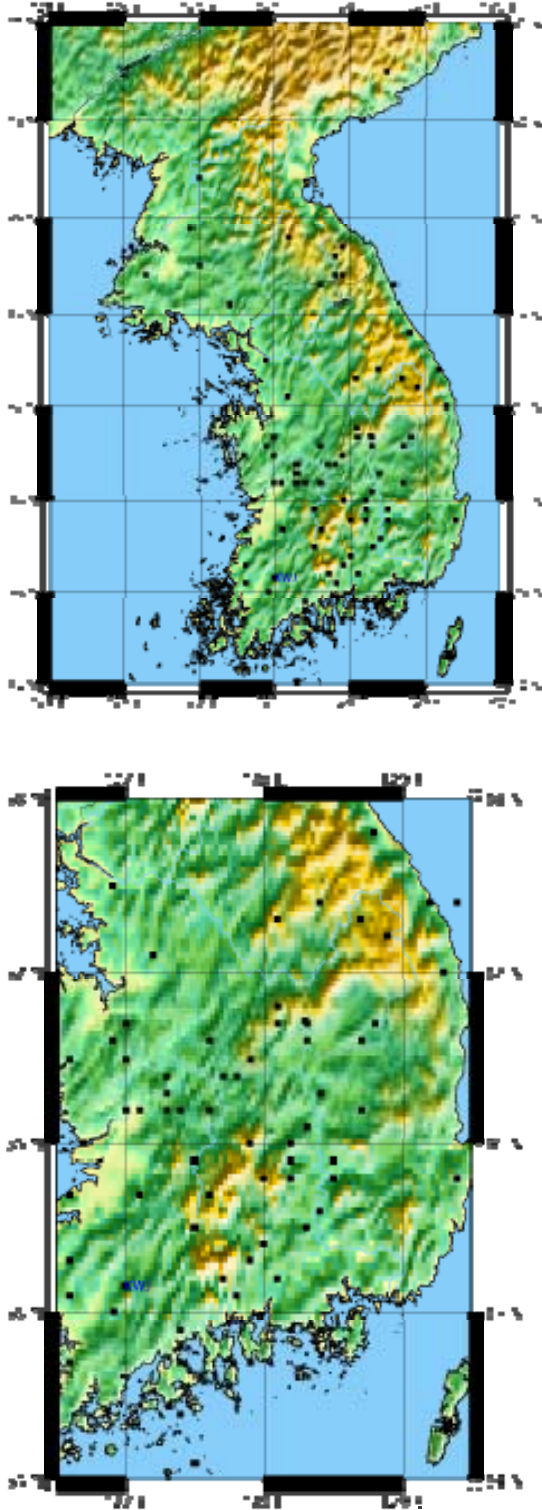


Figure 2. Map in the upper panel shows the event locations from which regional seismograms recorded by the KMA and KIGAM network stations (shown by solid squares, lower panel) have been archived. Seismograms have already been transformed to the necessary format for further processing.

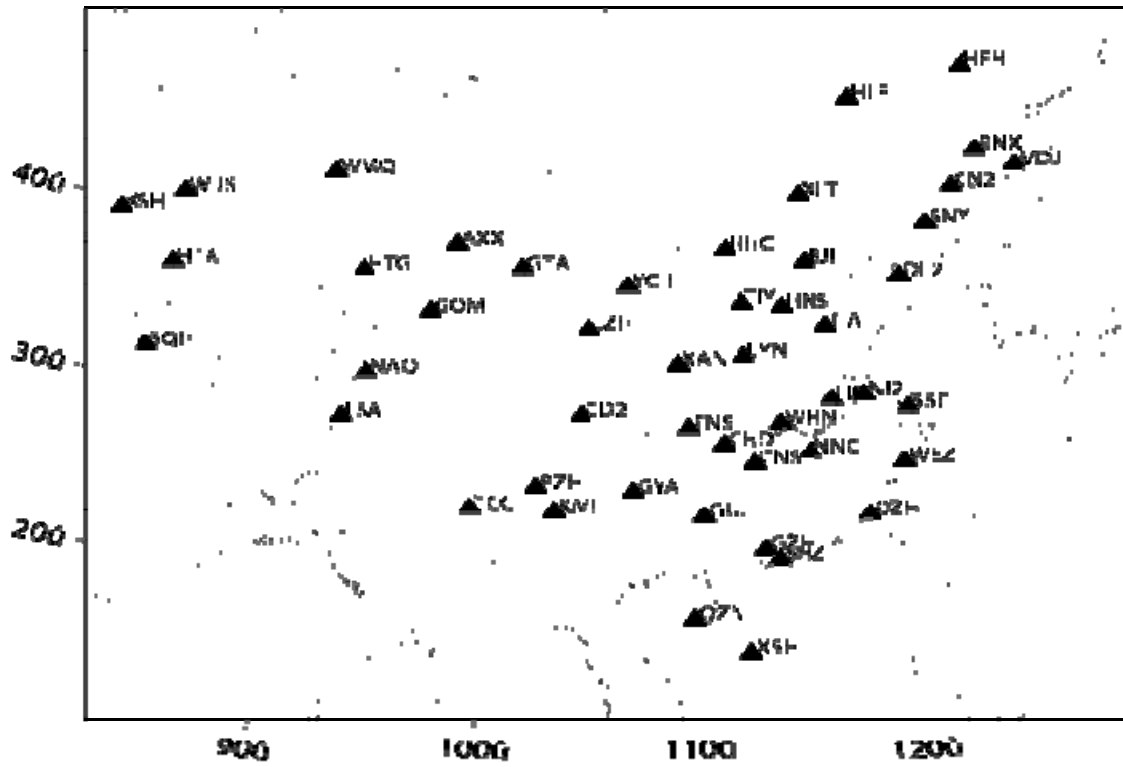


Figure 3. Station map of the CNDSN. Regional seismograms from this network have currently been modeled by our team member who is working collaboratively with the in-country scientists to investigate the crustal model in different parts of China. Using these data, seismic moment ( $M_o$ ) and moment-magnitude ( $M_w$ ) of many events have also been determined.

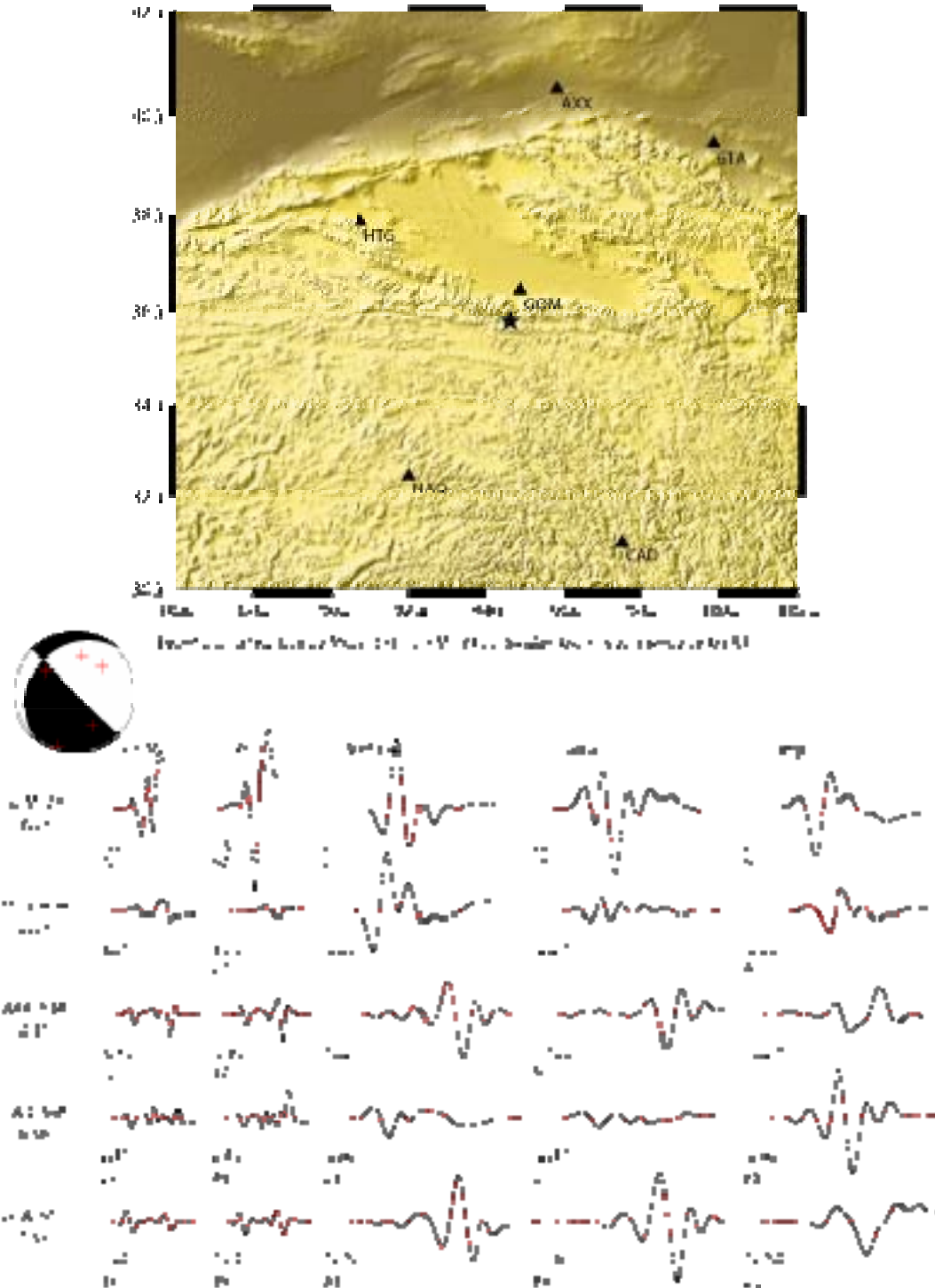


Figure 4. In top panel, the star represents the epicenter of a  $M_w$  5 aftershock of the 2001 Kunlun earthquake. Triangles are the nearby CNDNSN stations. The bottom panel shows modeling of the regional  $P_{nl}$  and surface wave seismograms yielding accurate focal parameters, seismic moment, and moment magnitude ( $M_w$ ).

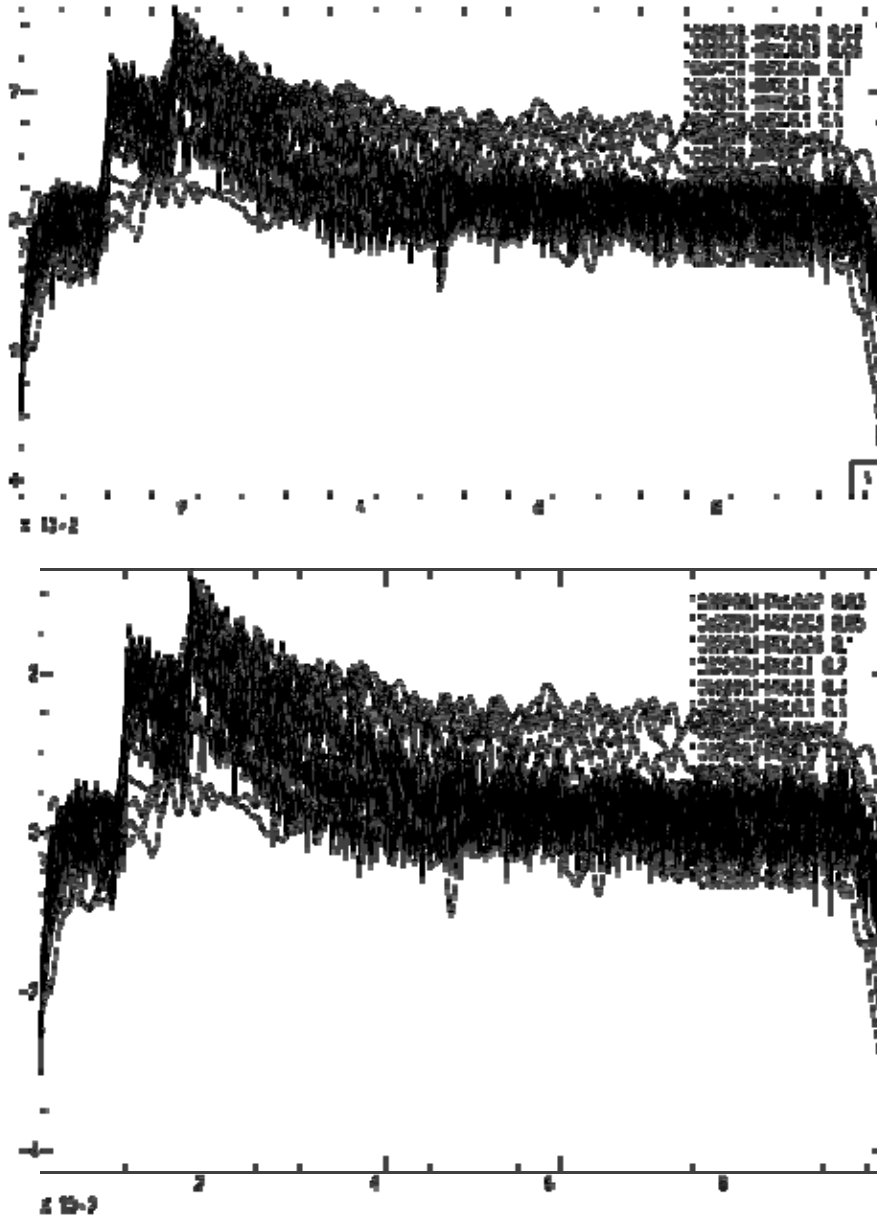


Figure 5. Envelopes processed using regional seismograms recorded at CNDSN station HTA at 14 different frequency bands from two separate events. Clearly, these envelopes show a straight-line decay between 2 and 4 Hz over which the coda magnitude can be measured.



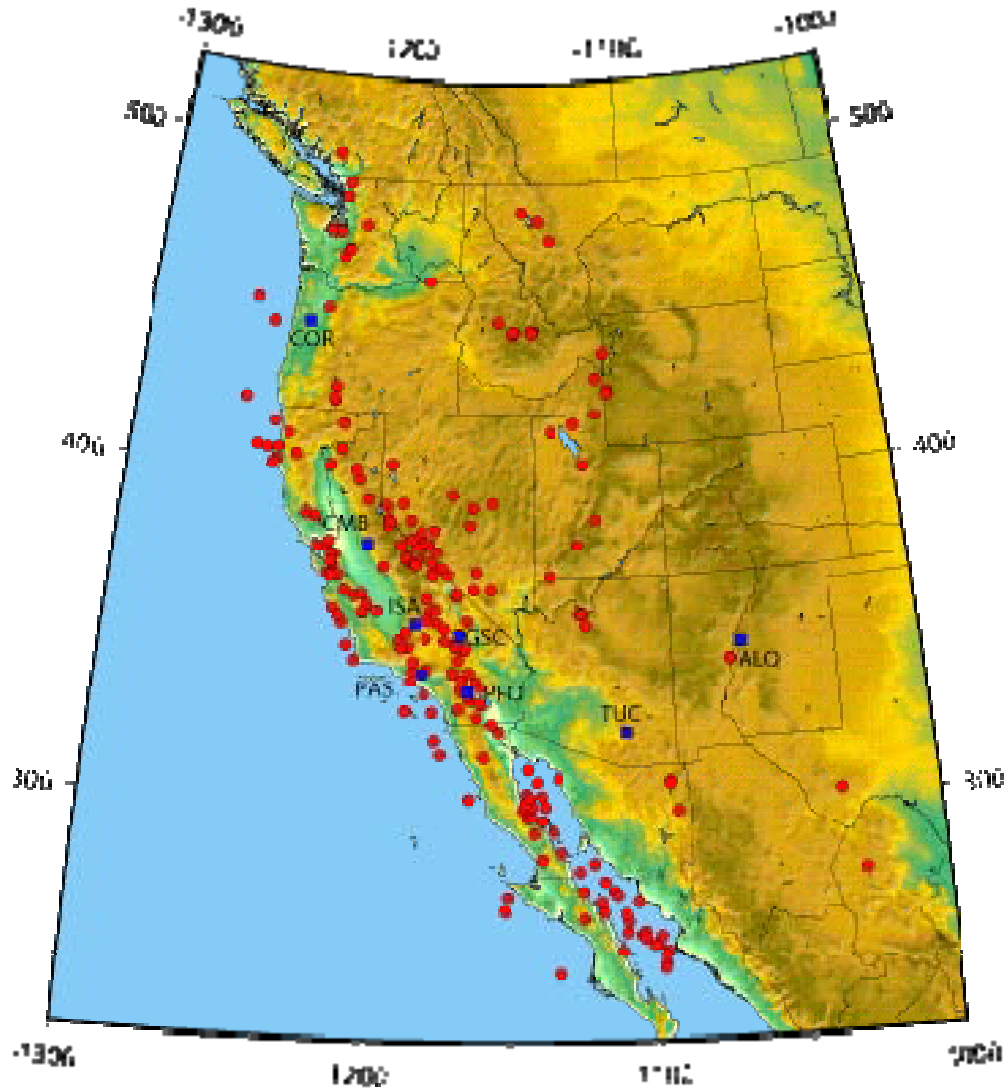


Figure 6. Map of the southwestern United States and bordering regions, showing the stations (blue squares) and earthquakes (red circles) used in a study to compare inter-station  $M_w$  (coda magnitude) and  $M_w$  (station-specific coda magnitude) vs  $M_w$  (moment-magnitude).

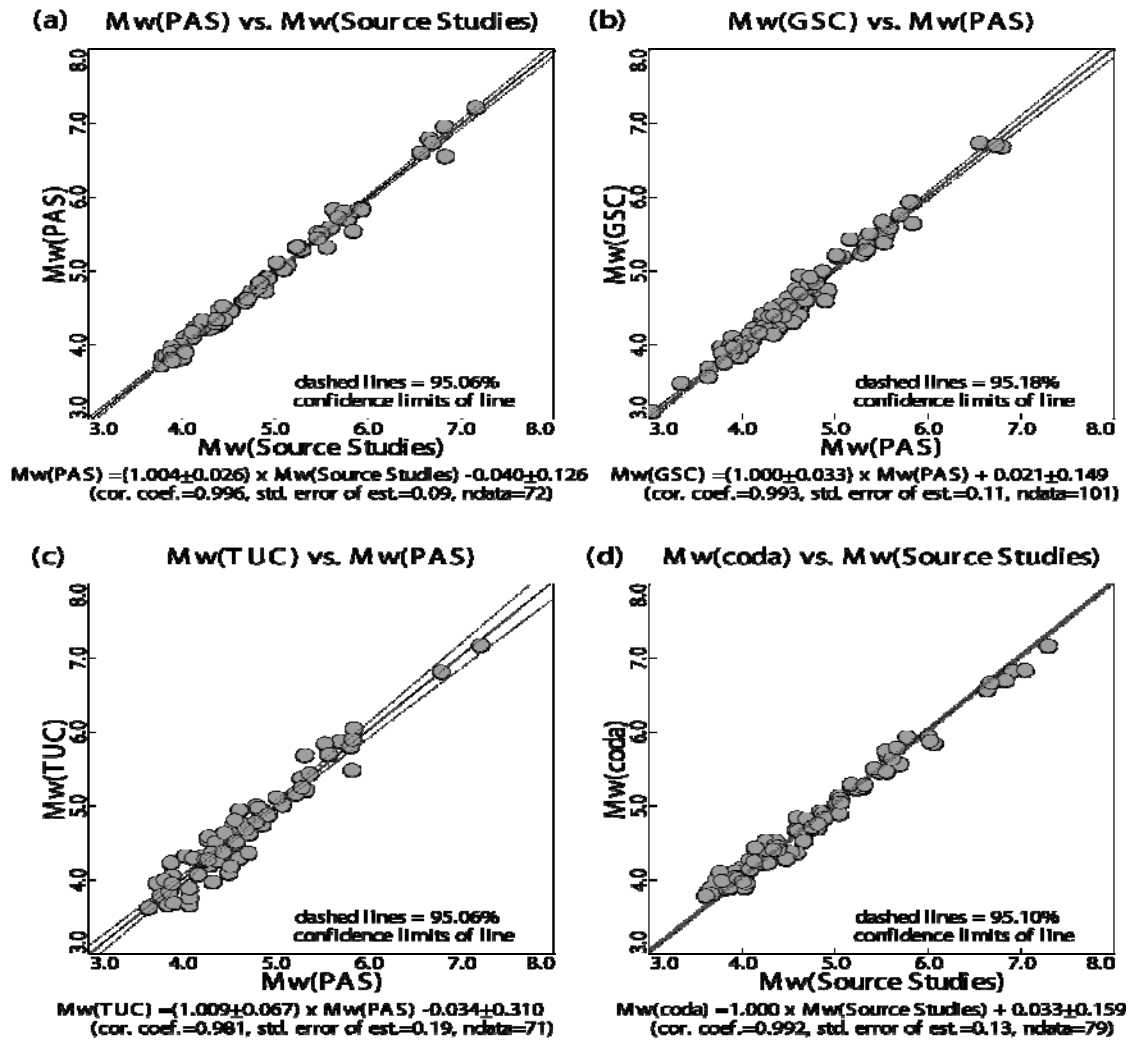


Figure 7.  $M_w(\text{coda})$  results for (a) single-station (PAS) vs  $M_w$  (source studies), (b) inter-station  $M_w(\text{coda})$  comparison for two relatively nearby stations GSC and PAS, (c) inter-station  $M_w(\text{coda})$  comparison for two distance stations TUC and PAS, and (d) network averaged  $M_w(\text{coda})$  vs  $M_w$  (source studies).  $M_w$  (source studies) is the moment-magnitude estimated using waveform modeling.